15 Apr 2014

The Properties And Structure Of Zinc Magnesium Phosphate Glasses

Charmayne E. Smith (Lonergan)
Missouri University of Science and Technology, clonergan@mst.edu

Richard K. Brow
Missouri University of Science and Technology, brow@mst.edu

Recommended Citation

The properties and structure of zinc magnesium phosphate glasses

Charmayne E. Smith, Richard K. Brow *

Missouri University of Science and Technology, Department of Materials Science & Engineering, Rolla, MO 65409, USA

A B S T R A C T

Zn–Mg-phosphate (ZMP) glasses, including those with the nominal molar compositions $(50 - x)ZnO \cdot xMgO \cdot 50P_2O_5$ $(0 \geq x \geq 50)$ and $(60 - y)ZnO \cdot yMgO \cdot 40P_2O_5 (0 \geq y \geq 60)$, were prepared and properties such as density, refractive index, coefficient of thermal expansion and glass transition temperature (T_g), were measured. The glass transition temperature increases by 100–150 °C and the room temperature dissolution rates in water decrease by 1–2 orders of magnitude when MgO replaces ZnO while maintaining a constant P_2O_5 content. Glass structures were characterized by Raman spectroscopy and there were no significant changes in the phosphate anion distributions when MgO replaces ZnO. The significant changes in properties cannot be explained by a simple cation field strength argument since Mg^{2+} and Zn^{2+} have similar sizes; instead, the effect of 3d electrons on the nature of the bonds between Zn^{2+} ions and non-bridging oxygens on the phosphate tetrahedra must be considered.

1. Introduction

Zinc phosphate glasses have been developed for use as LED light sources [1], and as substrates for optical waveguides written by f-sec lasers [2–5]. These glasses possess a UV-edge below 400 nm, which is useful for some optical applications [6]. Zinc phosphate glasses also tend to have greater coefficients of thermal expansion with low processing temperatures, which make them useful as sealing glasses [7,8].

A drawback to the use of binary zinc phosphate glasses is their susceptibility to chemical attack because of the ease of hydrolysis of the P–O–Zn bonds [9]. It is known that the incorporation of additional oxides can improve the chemical durability of phosphate glasses; one in particular is magnesium oxide which has been shown to reduce corrosion rates in aqueous solutions of zinc phosphate glasses, presumably due to the formation of more chemically resistant P–O–Mg bonds [10].

The properties and structures of binary zinc [9,11–24] and magnesium phosphate [14,18,25–30] glasses have been studied. Both the $ZnO–P_2O_5$ and the $MgO–P_2O_5$ binary systems have been classified as anomalous because of discontinuities in composition–property trends near the metaphosphate (50 mol% P_2O_5) composition [26]. Glasses from the $ZnO–P_2O_5$ binary have a minimum in T_g and CTE near 60 mol% ZnO [13], a behavior that is not found in the $MgO–P_2O_5$ system [19].

The addition of either ZnO or MgO to P_2O_5 results in systematic changes in properties that can be related to changes in the phosphate network structure. Phosphate anionic structures can be described using the Q^n-terminology, where 'n' represents the number of bridging oxygens on a phosphate tetrahedron [31]. For example, changes in the types of phosphate tetrahedra with the addition of MeO (where Me = Zn, Mg) can be described by the reaction:

$$2Q^n + MeO \rightarrow 2Q^{n-1}. \tag{1}$$

Binary phosphate glasses with increasing MeO-content (increasing O/P ratio) have shorter average phosphate anion lengths as nonbridging oxygens replace bridging oxygens on the P-tetrahedra. Evidence for these structural changes can be found in many spectroscopic studies, including Raman and/or infrared (IR) spectroscopies [11,25,28] and ^{31}P nuclear magnetic resonance (NMR) spectroscopy [20,32–34].

Khor and colleagues have described the effects of the composition of ternary zinc–magnesium-phosphate (ZMP) glasses on the optical, dielectric and physical properties [6,10,29,30,35]. They showed that the replacement of P_2O_5 by MgO decreases the aqueous dissolution rates of zinc phosphate glasses [10], although it is unclear if this improvement in chemical durability is due to the replacement of P–O–Zn bonds by P–O–Mg bonds, or to the overall decrease in the P_2O_5 content [9,36,37].

The goal of the present study is to determine the effects of substituting MgO for ZnO, while maintaining a constant P_2O_5 content (constant O/P ratio), on the properties and structures of zinc phosphate glasses, including compositions originally developed as substrates for femto-second processing [2]. A constant O/P ratio fixes the average chain length of the phosphate units in the structure [31] and so property changes can then be related to the nature of the P–O–Me bonds that link neighboring anions. The intent of this paper is to report the glass-forming ranges of several series of $ZnO–MgO–P_2O_5$ compositions, to describe the property trends due to the systematic replacement of ZnO by MgO, and to relate those property trends to the nature of the glass structures.

* Corresponding author.
E-mail address: brow@mst.edu (R.K. Brow).

2. Experimental

The glasses were prepared by mixing appropriate amounts of MgO (Alfa Aesar, 96%), $NH_4H_2PO_4$ (ACS, 98.0% − Alfa Aesar), and ZnO (reagent grade, ≥99.0% − Sigma Aldrich), calcining the batches in an alumina crucible for ~15 h. at 500 °C, then melting the batches between 1000 and 1500 °C for approximately 2 h in air. Melts were quenched on copper plates, and these glasses were remelted in the alumina crucibles using similar conditions to improve glass homogeneity. The final glass samples were obtained by pouring the melts into a steel mold (10 mm in diameter and 2.5 cm tall), or splat quenching between copper plates if necessary, and annealing near T_g for approximately two hours, before slowly cooling to room temperature.

The density of each bubble-free glass was measured using Archimedes' method with distilled water as the buoyancy liquid. Three samples of each glass were measured and the standard deviation is reported as the experimental uncertainty. The molar volume (MV) was calculated by dividing the density of each glass by the molecular weight, calculated from analyzed glass compositions. The compositions of polished samples were calculated from cation ratios determined using energy dispersive spectroscopy (EDS, Helios NanoLab 600 FIB/FESEM with an Oxford EDS attachment). The compositional uncertainty was determined by analyzing three or more areas of at least three different samples of the same composition and was found to be a maximum of ±0.6 mol% for each oxide [Table 1]. The glasses will be described using their nominal compositions, unless otherwise noted.

Differential thermal analysis (DTA, Perkin-Elmer DTA7) was used to determine the glass transition temperature (T_g) by heating 30–40 mg of glass powder (<75 μm) in an open, alumina crucible at a rate of 10 °C/min in a nitrogen atmosphere; the onset temperatures for the glass transition were determined with the accompanying software and the estimated uncertainty is ±5 °C.

The refractive indices (n) were measured using a prism coupler (Metricon model 2010/M) at 632.8 nm on samples that were ~1 mm thick and polished to a 1 μm finish (diamond paste, Allied High Tech); the uncertainty of these measurements is ±0.0004.

The dilatometric softening temperature (T_d) and the coefficient of thermal expansion (CTE) were determined using an Orton dilatometer (Model 1600D) on cylindrical samples approximately 2.54 cm in length, heated at a rate of 10 °C/min in air. The T_d is established as the maximum of the dilatometric data with a reproducibility of ±5 °C. The CTE is reported as the linear slope of data from 200 to 400 °C and these measurements were reproducible to ±0.2 ppm/°C.

Weight loss measurements from bulk glasses immersed in deionized (DI) water at 21 °C for up to 48 h were made to determine relative chemical durability. Polished disks (10 mm in diameter, 1 mm thick, 5 μm finish) were rinsed with acetone and dried before testing. A constant sample surface area (SA)-to-solution volume ratio of 0.035 cm^{-1} was used for each experiment. Samples were removed periodically from the polypropylene containers used for the corrosion tests, dried and weighed, and then returned to the original solution. Three samples were tested for each condition and the average weight loss and standard deviation are reported. Dissolution rates are reported as the linear slope of the weight loss data over the entire 48 h of each experiment.

Raman spectra were collected from a polished sample of each glass using a Jobin–Yvon micro-Raman spectrometer with a 632.8 nm He–Ne laser (17 mW) as the excitation source.

3. Results

3.1. Glass-forming region

The as-batched and measured compositions of the glasses are given in Table 1 and are shown in Fig. 1 along with other compositions melted to confirm the glass-forming region. Small amounts of alumina (<5 mol%) were dissolved into the glasses because of reactions between the melts and the alumina crucibles (Table 1). The binary magnesium phosphate glass with an intended O/P ratio of 3.25 had the largest alumina content (4.7 mol%) because of the high melting temperature used (1500 °C). P_2O_5-loss from the melts was limited and so compositions are grouped by their nominal O/P ratios. Glasses with an O/P ratio below 2.8, in the ultraphosphate region, were not prepared in this study. Studies of binary compositions prepared by traditional splat-quenching methods produced glasses with up to ~71 mol% ZnO [11,19,21] and ~65 mol% MgO [18,25,27,29]; these compositions coincide with the glass-forming ranges found in this work (Fig. 1).

The binary compositions with 70–80 mol% MgO were melted below 1500 °C, but the melts had very low viscosities and crystallized immediately upon quenching. The use of roller quenching has been shown to push the glass forming region of binary phosphate glasses with both ZnO [17] and MgO [28] up to 80 mol% and these reported roller-quenching limits of glass formation for the respective binaries are also shown in Fig. 1.

3.2. Physical and thermal properties

The densities of ZMP glasses with O/P ratios = 3.0 and 3.25 are shown in Fig. 2a and their molar volumes are shown in Fig. 2b. Also shown are the respective properties of glasses with similar compositions reported in the literature. For glasses with similar O/P ratios, the replacement of ZnO by MgO systematically decreases the density but has no significant effect on molar volume. Glasses with greater P_2O_5 contents (lower O/P ratios) have lower densities and greater molar volumes. Fig. 3a and b shows that the glass transition temperatures (T_g) and dilatometric softening temperatures (T_d), respectively, increase systematically with the replacement of ZnO by MgO, and do not vary significantly with O/P ratio. Fig. 4 shows that there is a small increase in the coefficients of thermal expansion (CTE) as a function of

Table 1
Nomenclature and compositions of the zinc magnesium phosphate glasses.

| Designation (mol%)	Batched compositions (mol%)	Measured analyzed compositions [mol%]				
ZMP_mol% MgO_O/P	ZnO–MgO–P_2O_5 [O/P ratio]	ZnO (±0.6)	MgO (±0.5)	P_2O_5 (±0.3)	Al_2O_3 (±0.2)	O/P
ZMP_0_3.0	50–0–50 [3.0]	48.5	0	49.4	2.1	3.05
ZMP_13_3.0	37.5–12.5–50 [3.0]	37.3	12.0	48.9	1.8	3.06
ZMP_25_3.0	25–25–50 [3.0]	25.0	23.4	50.0	1.6	3.03
ZMP_38_3.0	12.5–37.5–50 [3.0]	13.1	35.0	51.1	0.9	3.00
ZMP_50_3.0	0–50–50 [3.0]	0	46.1	53.1	0.8	2.96
ZMP_0_3.25	60–0–40 [3.25]	60.5	0	36.7	2.8	3.44
ZMP_15_3.25	45–15–40 [3.25]	38.7	19.1	41.2	1.0	3.24
ZMP_30_3.25	30–30–40 [3.25]	30.3	27.8	41.3	0.6	3.23
ZMP_45_3.25	15–45–40 [3.25]	15.5	42.0	41.6	0.9	3.22
ZMP_60_3.25	0–60–40 [3.25]	0	55.5	39.8	4.7	3.37
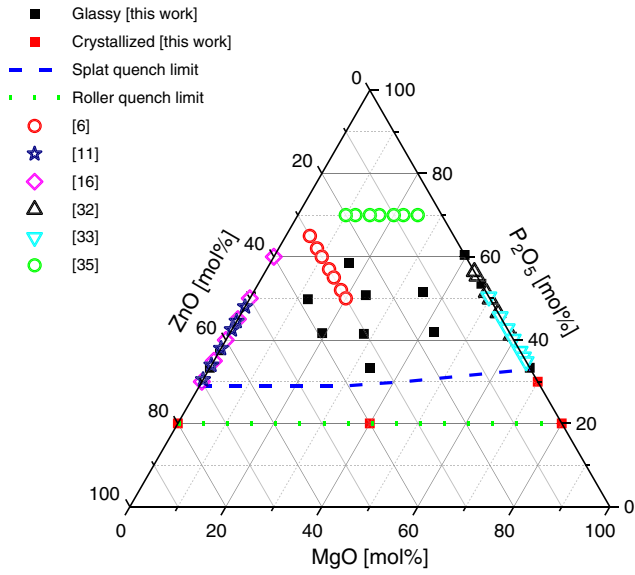
Fig. 1. Glass forming diagram of the zinc magnesium phosphate system. The blue dashed line indicates the glass forming range for splat quenching melts [this work] and the green dotted line is the estimated glass forming range for roller quenching. The diagram includes glass compositions reported in the literature [6,11,16,32,33,35].
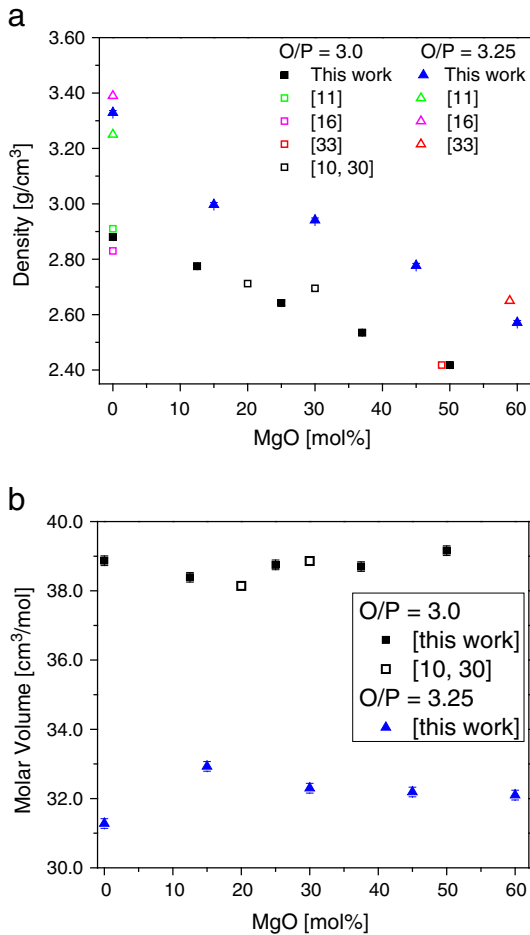

Fig. 3. a) The glass transition temperatures and b) dilatometric softening temperatures [error = ±5 °C] for the ZMP glasses with O/P = 3.0 [squares] and 3.25 [triangles]. Data from the literature are given as open symbols.

MgO content, and glasses with O/P = 3.25 have slightly greater CTEs than glasses with O/P = 3.0.

The refractive indices measured at 632.8 nm are shown in Fig. 5. With the replacement of ZnO by MgO, there is a systematic decrease in the refractive index. Glasses with greater P_2O_5 contents (lower O/P ratios) have lower refractive indices for glasses with similar MgO-contents.

Fig. 2. a) Density and b) molar volume of ZMP glasses with O/P = 3.0 [squares] and 3.25 [triangles]. Data from the literature are given as open symbols.
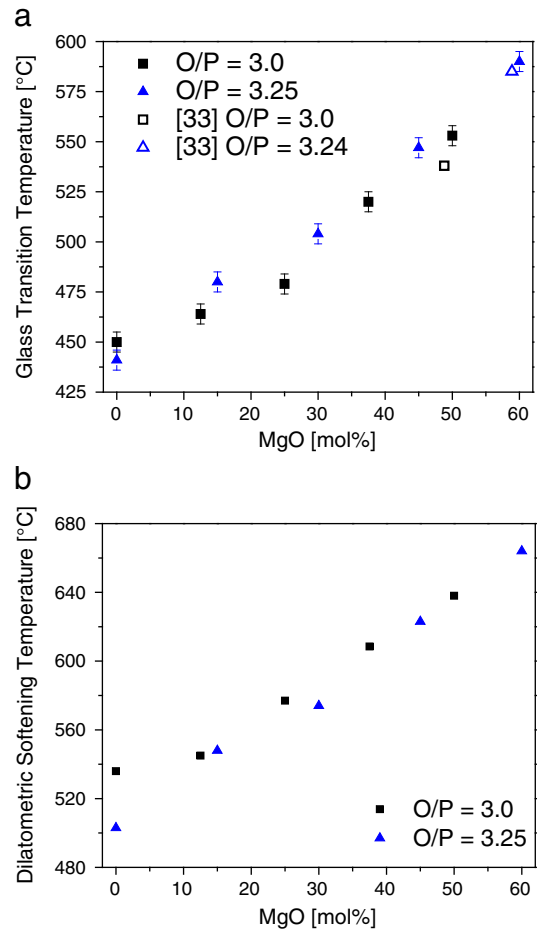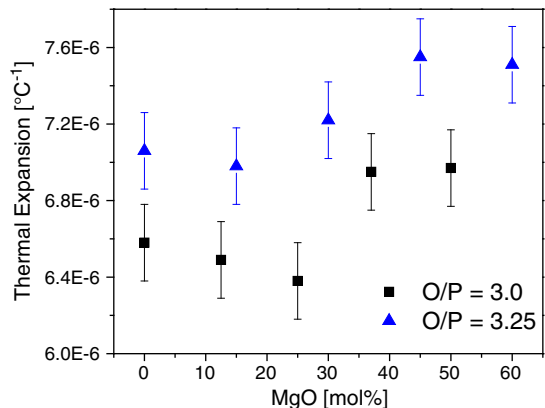

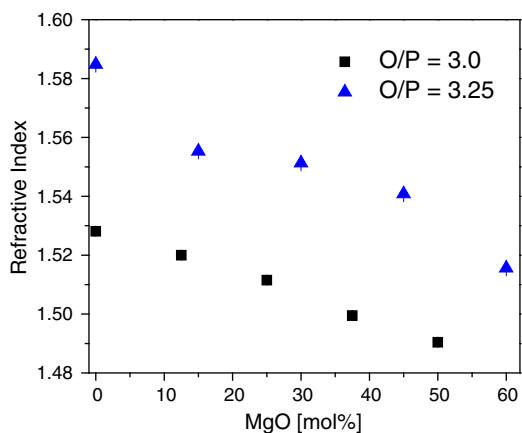**Fig. 4.** Coefficient of thermal expansion for the ZMP glasses.

Fig. 5. Refractive indices (at 632.8 nm) of glasses in the ZnO–MgO–P$_2$O$_5$ system.

3.3. Chemical durability

The data for weight loss in room temperature water for the ZMP glasses with O/P ratios of 3.0 and 3.25 are shown in Fig. 6a and b, respectively. In general, the glasses exhibit a linear weight loss behavior over the 48 h of the tests. There is an overall decrease in weight loss rate with the replacement of ZnO by MgO in the composition, as can be seen in Fig. 6c. The exception is the relatively low weight loss rate for the glass with the nominal molar composition 60ZnO–40P$_2$O$_5$.

3.4. Raman spectroscopy

The Raman spectra of the metaphosphate (O/P = 3.0) and polyphosphate (O/P = 3.25) glasses are shown in Fig. 7a and b, respectively.

Raman spectra of the binary zinc phosphate glasses are comparable to spectra from similar compositions reported in the literature [11]. The spectrum from the 50MgO–50P$_2$O$_5$ glass also is similar to a previously reported spectrum of similar glass, but the spectrum from the 60MgO–40P$_2$O$_5$ glass is more similar to that reported for a glass with a greater MgO content (65MgO–35P$_2$O$_5$) [38], likely due to the relatively large alumina content (4.7 mol%) in the present glass.

The Raman spectra of glasses in the metaphosphate compositional range have the following features: peaks near 700 cm^{-1} and 1200 cm^{-1}, and a broad shoulder in the range 1240–1350 cm^{-1}; these peaks are assigned to the POP$_{sym}$ stretching mode of bridging oxygens in Q^2 units, the (PO$_2$)$_{sym}$ stretching mode of non-bridging oxygens in Q^2 units, and the (PO$_2$)$_{asym}$ stretching mode of non-bridging oxygens in Q^2 units, respectively [11,23]. When MgO replaces ZnO in this series (Fig. 7a), the main peak at 1200 cm^{-1} narrows slightly and shifts to a greater frequency (discussed below); in addition, the peak near 1282 cm^{-1} becomes more distinct and intense.

The Raman spectra for the ZMP polyphosphate glasses (O/P = 3.25), shown in Fig. 7b, have peaks at ~700 cm^{-1}, an intense peak at 1200 cm^{-1} and a broad shoulder centered near 1310 cm^{-1}, similar to what was observed in the spectra from the metaphosphate glasses. In addition, there is a shoulder at ~750 cm^{-1} due to the POP stretching mode associated with Q^1 sites and a broad shoulder centered near ~1050 cm^{-1} that is due to the (PO$_3$)$_{sym}$ stretching modes of nonbridging oxygens in Q^1 tetrahedra [11,23]. There are no significant changes in the shapes of the Raman spectra of the ZMP polyphosphate glasses when MgO replaces ZnO; however, there are systematic shifts in the peak positions (discussed below). The relative intensity of the shoulder between 900 and 1100 cm^{-1} in the spectrum from the 60MgO–40P$_2$O$_5$ glass is greater than it is in the spectra from the other glasses and this is related to the greater O/P ratio measured for this glass (3.44, Table 1) than for the others.
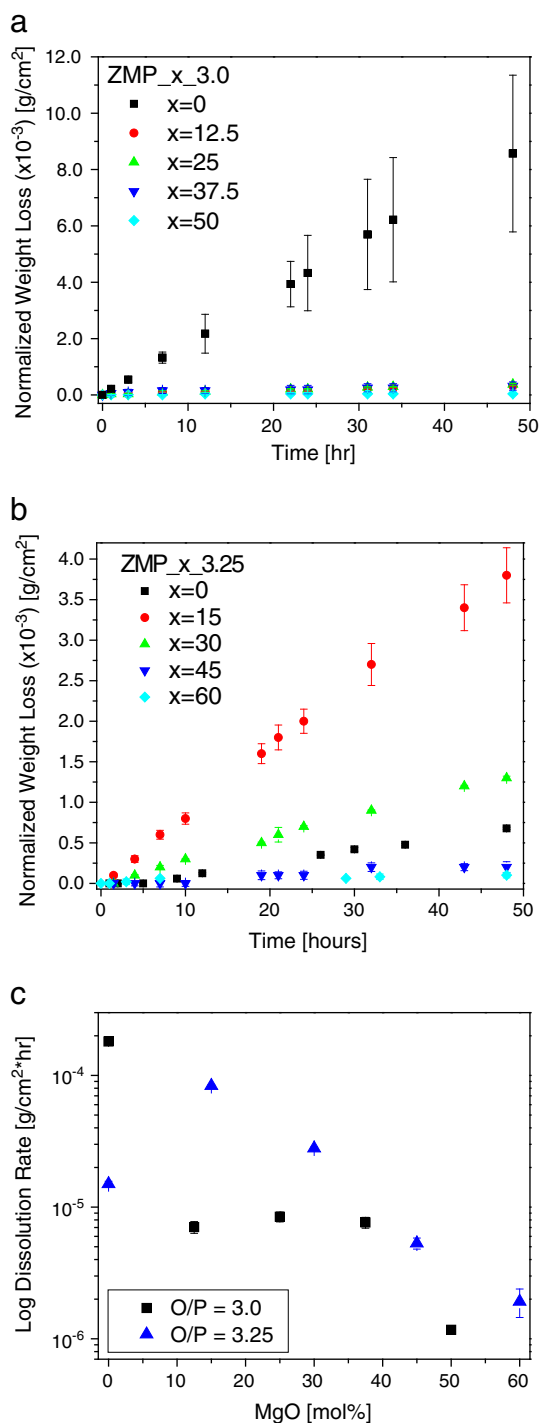

Fig. 6. Weight loss data in room temperature water for ZMP glasses with a) O/P = 3.0 and b) O/P = 3.25; c) dissolution rates calculated from the weight loss data over 48 h.

4. Discussion

4.1. Glass properties

The decrease in density with the replacement of ZnO by MgO (Fig. 2a) is due to the smaller mass of Mg compared to Zn. The molar volumes of the two series (Fig. 2b), however, show no significant changes with MgO substitution; this indicates that there is no significant structural reorganization in the respective glasses when MgO replaces ZnO. There is a significant decrease in molar volume for glasses with greater O/P ratios. Some of the variability in the molar volumes
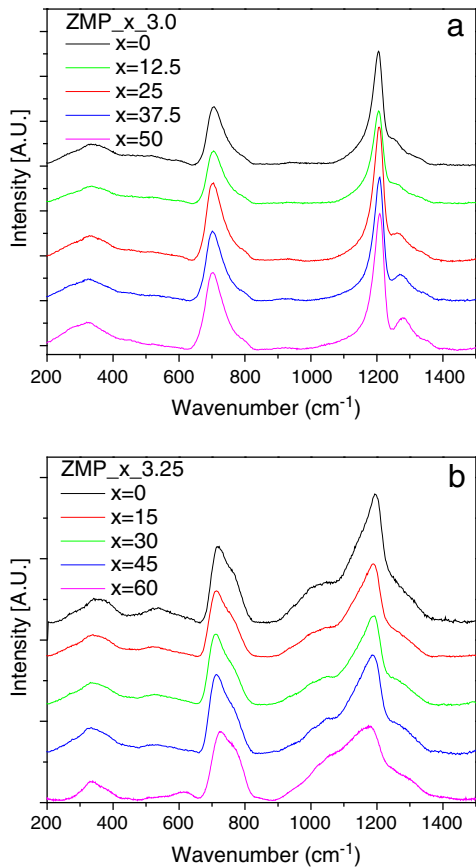
Fig. 7. Raman spectra of ZMP glasses with a) O/P = 3.0 and b) O/P = 3.25.

of glasses within a series may be due to small variations in O/P ratios due to differences in the residual alumina content and P_2O_5 volatility during melting.

The lower molar volumes for the zinc–magnesium polyphosphate (O/P = 3.25) glasses compared to the metaphosphate (O/P = 3.00) glasses are consistent with the smaller phosphate anions associated with the former series. For both the binary Zn- and Mg-phosphate glasses, there is a systematic decrease in the molar volumes with increasing O/P ratios (Fig. 8). The Raman spectra of the ZMP glasses are consistent with the formation of smaller phosphate anions with increasing O/P ratios, following Eq. (1). The smaller average phosphate
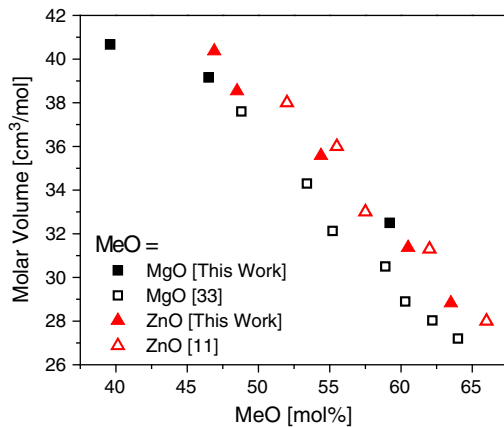
anions, and the larger relative fractions of Zn- and Mg-polyhedra, pack more efficiently in the structures of glasses with greater O/P ratios, decreasing the overall molar volume of these glasses. These trends are consistent with those reported by Walter et al., who noted increases in packing densities with increasing O/P ratios for binary Mg-phosphate glasses [33] and for binary Zn-phosphate glasses [19].

The replacement of ZnO by MgO in the ZMP glasses decreases the refractive index with increasing MgO for both O/P ratio series (Fig. 5), which is in agreement with previous studies [35], and is explained by the greater ionic refractivity (R_i) of Zn^{2+} ($R_i = 0.70$) compared to Mg^{2+} (0.25) and P^{5+} (0.05) [39]. Molar refraction (R_m) values were calculated from the measured refractive indices and calculated molar volumes (MV) from the Lorenz–Lorentz equation [40]:

$$R_m = MV \cdot \frac{\left(n^2 - 1\right)}{\left(n^2 + 2\right)}. \tag{2}$$

As shown in Fig. 9a, molar refraction decreases when MgO replaces ZnO in both series of glasses, indicating an overall decrease in the polarizability of the Mg-rich glasses. The individual ionic contributions to R_m can be determined from the ion concentrations (c_i) and individual ionic refractivities from [39]:

$$R_m = \sum_i R_i \cdot c_i. \tag{3}$$

Assuming constant ionic refractivities for all cations (including Al^{3+}), the oxygen refractivity can then be determined from the values

Fig. 8. Molar volume plotted as a function of MeO content for binary MeO–P_2O_5 glasses [Me = Zn (red triangles) or Mg (black squares)] from this work. Data from the literature are shown as open symbols.
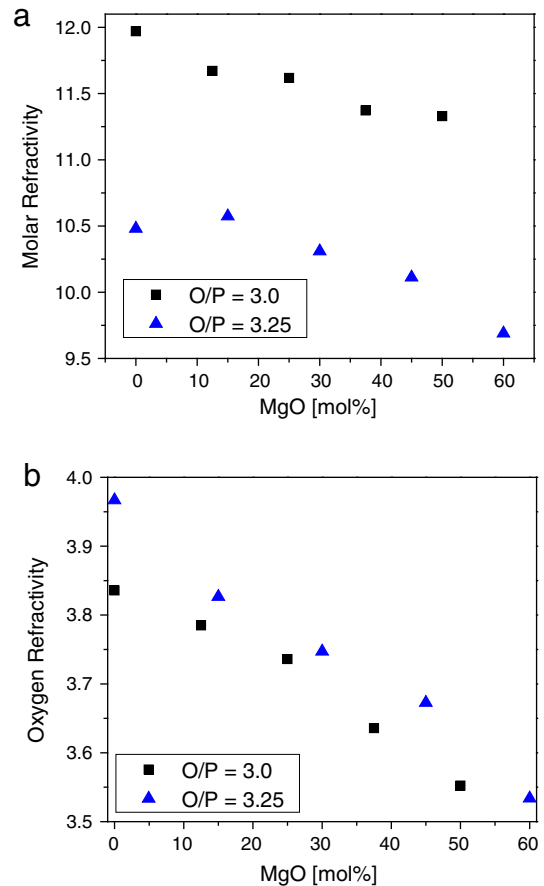

Fig. 9. a) Molar refractivity and b) oxygen refractivity of ZMP glasses with O/P = 3.0 (black squares) and 3.25 (blue triangles).

of R_m and the measured glass compositions (Table 1). The oxygen refractivities are shown as a function of MgO content for both O/P ratio series in Fig. 9b. The systematic decrease in oxygen refractivity indicates that there is a decrease in the polarizability of the average nonbridging oxygen when MgO replaces ZnO in both series of glasses. The oxygen refractivities of the polyphosphate glasses are greater than those of the metaphosphate glasses because the former have a greater fraction of more polarizable nonbridging oxygens.

The replacement of ZnO by MgO has a significant effect on the glass transition (Fig. 3a) and the dilatometric softening temperatures (Fig. 3b). The thermal properties of phosphate glasses are often discussed in terms of the relative field strengths (charge/(ionic radius)^2) of the cations added. High field strength cations, like Al^{3+}, form strong bonds with the non-bridging oxygens on the phosphate anions [41,42] and these bonds have a great effect on thermal properties. Metwalli et al., reported an increase in T_g of ~200 °C with the replacement of MgO by Al_2O_3 for a series of metaphosphate glasses with a constant O/P ratio [43]. The field strength argument, however, does not explain the large increase in T_g when MgO replaces ZnO because these two cations have the same charge and similar sizes: in tetrahedral sites, 0.071 nm for Mg^{2+} and 0.074 nm for Zn^{2+} [44].

The systematic changes in glass properties with the replacement of ZnO by MgO should be understood by the differences in ion properties other than size. Weyl and Marboe have noted that oxide melting temperatures can be affected by a few key factors, i.e. differences in cation charge, anion size to cation size ratio, cation size and ion polarizability [45]. Mg^{2+} and Zn^{2+} have similar sizes and the same charge, but have different polarizabilities, as reflected by their different ionic refractivities. A comparison of the melting temperatures of ZnO (1975 °C) and MgO (2800 °C) shows that cation polarizability has a strong effect on thermal properties and it has been noted before that oxides of cations with noble-gas configurations (MgO) tend to have greater melting temperatures than oxides with d-electrons in their outer shells (ZnO) [45]. The $3d^{10}$ electrons contribute to the greater polarizability of Zn^{2+}, compared to Mg^{2+}. The greater shielding effects of the d-electrons lead to weaker coulombic interactions with neighboring anions. The stronger coulombic interactions between Mg^{2+} and nonbridging oxygens on a phosphate tetrahedron, compared with Zn^{2+}, leads to the significant increase in the glass transition (Fig. 3a) and dilatometric softening (Fig. 3b) temperatures when MgO replaces ZnO for both O/P ratio series. These trends in the characteristic temperatures of the glasses are also consistent with the melting points of the respective crystalline compounds: $Mg(PO_3)_2$ (1160 °C) [46] and $Zn(PO_3)_2$ (872 °C) [47], and $Mg_3(PO_4)_2$ (1357 °C) and $Zn_3(PO_4)_2$ (1060 °C) [46].

4.2. Chemical durability

The linear trends in weight loss with time are typical for the dissolution processes of many phosphate glasses in aqueous solutions [36,48]. When phosphate glasses react in water, the bonds between metal cations and non-bridging oxygens (P–O–Me) become hydrated. The bridging oxygen bonds (P–O–P) remain unbroken and only the nonbridging oxygen sites of the structure are affected, releasing entire phosphate anions intact into the solution [15,49,50]. Thus the dissolution rates of phosphate glasses depend on the hydration rates of the interchain linkages. The replacement of P–O–Zn bonds by P–O–Mg bonds for glasses with similar O/P ratios produces a decrease in the dissolution rates of the ZMP glasses in water (Fig. 6c). This is consistent with the study by Khor et al., who also showed that the addition of MgO to zinc phosphate glasses decreased dissolution rates [10], although the decrease noted in their work could also be the result of the concomitant replacement of P_2O_5 by MgO and ZnO.

The overall decrease in dissolution rates when MgO replaces ZnO indicates that the P–O–Mg bonds are more resistant to hydration than the P–O–Zn bonds. Takebe et al. [51] have related the relative dissolution rates of binary phosphate glasses to the polarizability of the

nonbridging oxygens in the P–O–Me bonds that link neighboring P-anions. They proposed that the more polarizable bonds react more readily with water to reduce the overall chemical durability. If the oxygen refractivity data in Fig. 9b is a measure of the relative polarizability of P–O–Zn and P–O–Mg bonds, then replacing ZnO with MgO reduces the average polarizability of oxygens in the glass and so, from the Takebe mechanism, would make the glass less reactive in water.

It should be noted that the 60MgO–40P$_2$O$_5$ glass has a much lower dissolution rate (1.5×10^{-5} g/cm^2 * h) than several others in the polyphosphate series. A white corrosion film formed on this sample (inset to Fig. 10) that did not form on any other sample. The film was X-ray amorphous, but Raman spectroscopy (Fig. 10) indicates that it has a chemical structure that is similar to the crystalline compound $Zn_2P_2O_7$. Zinc phosphate glasses have been reported to exhibit two different dissolution behaviors in water, either by progressive dissolution and the precipitation of material in solution (Type I) or by dissolution and the formation of a precipitation layer on the reacting glass surface (Type II) [9]. The 60MgO–40P$_2$O$_5$ glass was the only sample to exhibit the Type II dissolution behavior, and the formation of the amorphous corrosion layer appears to have reduced the overall dissolution rate of this glass.

4.3. Glass structure

It is important to recall that the trends in thermal and chemical properties of the ZMP glasses are not associated with significant reorganization of the phosphate network structure. There are no significant changes in the molar volumes of the glasses, and the Raman spectra are similar within each glass series when MgO replaces ZnO. There are systematic changes in the Raman peak positions. For the metaphosphate (O/P = 3.0) series, the peak for the PO_2 symmetric stretching mode near 1200 cm^{-1} increases in frequency with increasing MgO (Fig. 11). The peak for the PO_2 asymmetric stretching mode also increases in frequency, from the shoulder near 1247 cm^{-1} from the Zn-metaphosphate glass to the sharp peak at 1282 cm^{-1} for the Mg-metaphosphate glass [Fig. 7a]. Popovic et al. [52] and Nelson et al. [53] relate these increases in frequency to a decrease in the average P–nonbridging oxygen bond lengths. This is consistent with diffraction studies which show that the P–NBO bond length in a Mg-metaphosphate glass is shorter (0.149 ± 0.001 nm [33]) than that in a Zn-metaphosphate glass (0.150 ± 0.002 nm [12]).

For the series of ZMP glasses with an O/P ratio = 3.25, there is a significant decrease in the frequency of the $(PO_2)_{sym}$ stretching mode (Fig. 11a) and an increase in the frequency of the $(PO_3)_{sym}$ stretching mode with increasing MgO. Using the Popovic correlation [52], these
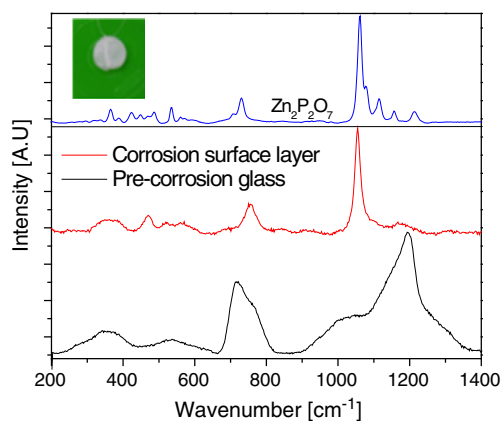

Fig. 10. Raman spectra of the 60MgO–40P$_2$O$_5$ glass surface before (bottom) and after (middle) 48 h in room temperature water, compared to the spectrum from crystalline $Zn_2P_2O_7$ (top). The inset shows an optical image of this glass after corrosion testing.
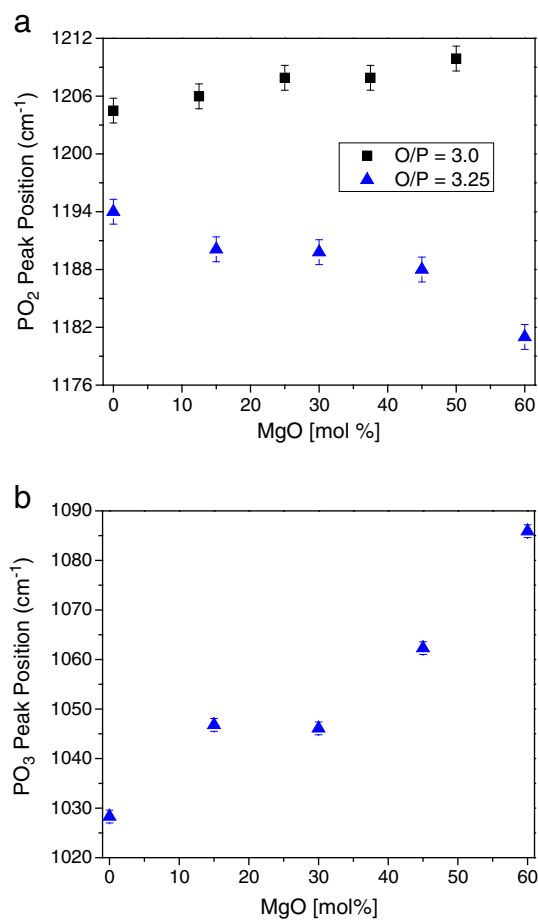
Fig. 11. Raman peak positions of the a) PO_2 symmetric stretching mode for ZMP glasses with O/P = 3.0 [black squares] and O/P = 3.25 [blue triangles], and b) PO_3 symmetric stretching mode for O/P = 3.25.

trends in respective peak positions indicate that the average P-NBO bond lengths associated with Q^2 units are getting longer and the average P – NBO bond lengths associated with the Q^1 units are becoming shorter as MgO replaces ZnO in the polyphosphate glass series. The shorter P – O bonds on the Q^1 tetrahedra are consistent with the lower average polarizabilities of the oxygen ions, implied by the lower oxygen ionic refractivity shown in Fig. 9b.

The shorter P – NBO bonds on Q^2 tetrahedra for the metaphosphate series and shorter P – NBO bonds on Q^1 tetrahedra for the polyphosphate series may also explain the increases in glass transition (Fig. 3a) and dilatometric softening temperatures (Fig. 3b) as ZnO is replaced by MgO. Shorter bonds imply stronger bonds that may require more thermal energy to deform.

5. Conclusions

The properties and structures of ZnO–MgO–P_2O_5 glasses, where ZnO was systematically replaced by MgO, have been described. Zinc and magnesium ions have similar sizes and this compositional substitution has little effect on the molar volumes of the glasses and Raman spectroscopy indicates that these compositional changes do not significantly affect the overall phosphate network. However, substantial changes in glass properties, including increases by over 100 °C in the glass transition temperature and reductions by 1–2 orders of magnitude in aqueous dissolution rates, indicate that ZnO and MgO affect the glasses in different ways.

The $3d^{10}$ electrons associated with the Zn^{2+} ion make it more polarizable than the Mg^{2+} ion. This polarizability accounts for the greater ionic refractivity of Zn^{2+} and so for the greater refractive indices for the Zn-rich glasses. The $3d^{10}$ electrons also screen the zinc nucleus, reducing the Coulombic attraction between Zn^{2+} ions and nonbridging oxygens on phosphate tetrahedra compared to the Mg^{2+} ions, accounting for the systematic increases in T_g with MgO-substitution.

The average ionic refractivity of the oxygen ions decreases with increasing MgO-substitution, indicating that the non-bridging oxygens associated with the P – O – Mg bonds are becoming less polarizable. This lower polarizability may make the P – O – Mg bonds less susceptible to hydration reactions to account for the improved chemical durability of these glasses when MgO replaces ZnO.

Acknowledgments

References

[1] R. Martinez-Martinez, et al., White light generation through the zinc metaphosphate glass activated by Ce^{3+}, Tb^{3+} and Mn^{2+} ions, J. Lumin. 129 (11) (2009) 1276–1280.

[2] L.B. Fletcher, et al., Effects of rare-earth doping on femtosecond laser waveguide writing in zinc polyphosphate glass, J. Appl. Phys. 112 (2) (2012) (023109-023109-6).

[3] L.B. Fletcher, et al., Direct femtosecond laser waveguide writing inside zinc phosphate glass, Opt. Express 19 (9) (2011) 7929–7936.

[4] L.B. Fletcher, et al., Femtosecond laser writing of waveguides in zinc phosphate glasses, Opt. Mater. Express 1 (2011) 845–855.

[5] L. Canioni, et al., Three-dimensional optical data storage using third-harmonic generation in silver zinc phosphate glass, Opt. Lett. 33 (4) (2008) 360–362.

[6] S.F. Khor, et al., Optical properties of ternary zinc magnesium phosphate glasses, Ceram. Int. 38 (2012) 935–940.

[7] B.G. Aitken, et al., Non-lead sealing glasses (Patent US5246890), Corning Incorporated, United States, 1993.

[8] R.M. Morena, Phosphate glasses as alternatives to Pb-based sealing frits, J. Non-Cryst. Solids 263&264 (2000) 382–387.

[9] H. Takebe, et al., Dissolution behavior of ZnO–P_2O_5 glasses in water, J. Non-Cryst. Solids 352 (2006) 3088–3094.

[10] S.F. Khor, et al., Degradation study on ternary zinc magnesium phosphate glasses, J. Mater. Sci. 46 (2011) 7895–7900.

[11] R.K. Brow, et al., The short-range structure of zinc polyphosphate glass, J. Non-Cryst. Solids 191 (1995) 45–55.

[12] U. Hoppe, et al., Structure of zinc phosphate glasses probed by neutron and X-ray diffraction of high resolving power and by reverse Monte Carlo simulations, J. Non-Cryst. Solids 351 (2005) 1020–1031.

[13] T. Kubo, et al., Thermal properties and structure of zinc phosphate glasses, Phys. Chem. Glasses Eur. J. Glass Sci. Technol. B 50 (1) (2009) 15–18.

[14] E. Matsubara, et al., Structural study of binary phosphate glasses with MgO, ZnO, and CaO by X-ray diffraction, J. Non-Cryst. Solids 103 (1988) 117–124.

[15] B.C. Sales, et al., Structure of zinc polyphosphate glasses, J. Non-Cryst. Solids 226 (1998) 287–293.

[16] B. Tischendorf, et al., The structure and properties of binary zinc phosphate glasses studied by molecular dynamics simulations, J. Non-Cryst. Solids 316 (2003) 261–272.

[17] B. Tischendorf, et al., A study of short and intermediate range order in zinc phosphate glasses, J. Non-Cryst. Solids 282 (2001) 147–158.

[18] G. Walter, et al., Intermediate range order in MeO–P_2O_5 glasses, J. Non-Cryst. Solids 217 (1997) 299–307.

[19] G. Walter, et al., The structure of zinc polyphosphate glass studied by diffraction methods and ^{31}P NMR, J. Non-Cryst. Solids 333 (2004) 252–262.

[20] J.W. Wiench, et al., Structure of zinc polyphosphate glasses studied by two-dimensional solid and liquid state NMR, J. Mol. Struct. 602–603 (2002) 145–147.

[21] K. Suzuya, et al., The structure of binary zinc phosphate glasses, J. Non-Cryst. Solids 345&346 (2004) 80–87.

[22] K. Meyer, Characterization of the structure of binary zinc ultraphosphate glasses by infrared and Raman spectroscopy, J. Non-Cryst. Solids 209 (1997) 227–239.

[23] J. Schwarz, et al., "Physical properties of PbO–ZnO–P_2O_5 glasses". I. Infrared and Raman Spectra, J. Optoelectron. Adv. Mater. 6 (3) (2004) 737–746.

[24] M. Crobu, et al., Chain-length-identification strategy in zinc polyphosphate glasses by means of XPS and ToF-SIMS, Anal. Bioanal. Chem. 403 (2012) 1415–1432.

[25] K. Meyer, Structural characterisation of binary magnesium ultraphosphate glasses by vibrational spectroscopy, Phys. Chem. Glasses 42 (2) (2001) 79–87.

[26] E. Kordes, et al., Physikalisch-Chemische Untersuchaften Uber Die Eigenschaften Und Den Feinbau Von Phosphatglasern, Z. Elektrochem. 57 (4) (1953) 282–289.

[27] K. Suzuya, et al., The structure of magnesium phosphate glasses, J. Phys. Chem. Solids 60 (1999) 1457–1460.

[28] K. Meyer, et al., A study of the structure of binary magnesium ultraphosphate glasses by vibrational spectroscopy, Ceram. Silik. 43 (4) (1999) 169–174.

[29] S.F. Khor, et al., Effects of MgO on dielectric properties and electrical conductivity of ternary zinc magnesium phosphate glasses, J. Non-Cryst. Solids 355 (2009) 2533–2539.

[30] S.F. Khor, et al., Effects of ZnO on dielectric properties and electrical conductivity of ternary zinc magnesium phosphate glasses, Am. J. Appl. Sci. 6 (5) (2009) 1010–1014.

[31] R.K. Brow, Review: the structure of simple phosphate glasses, J. Non-Cryst. Solids 263&264 (2000) 1–28.

[32] F. Fayon, et al., ^{31}P NMR study of magnesium phosphate glasses, J. Non-Cryst. Solids 283 (2001) 88–94.

[33] G. Walter, et al., Structural study of magnesium polyphosphate glasses, J. Non-Cryst. Solids 320 (2003) 210–222.

[34] J.W. Wiench, et al., Structural studies of zinc polyphosphate glasses by nuclear magnetic resonance, J. Non-Cryst. Solids 263&264 (2000) 101–110.

[35] S.F. Khor, et al., Optical properties of ultraphosphate glasses containing mixed divalent zinc and magnesium ions, Opt. Mater. 35 (2013) 629–633.

[36] M.B. Tosic, et al., Dissolution behavior of a polyphosphate glass into an aqueous solution under static leaching conditions, J. Non-Cryst. Solids 362 (2013) 185–194.

[37] A.E. Marino, et al., Durable phosphate glasses with lower transition temperatures, J. Non-Cryst. Solids 289 (2001) 37–41.

[38] M.A. Karakassides, et al., Preparation and structural study of binary phosphate glasses with high calcium and/or magnesium content, J. Non-Cryst. Solids 347 (2004) 69–79.

[39] I. Fanderlik, Optical properties of glass, Glass Science and Technology, 5, Elsevier, New York, 1983.

[40] J.A. Duffy, The refractivity and optical basicity of glass, J. Non-Cryst. Solids 86 (1986) 149–160.

[41] N.H. Ray, Composition–property relationships in inorganic oxide glasses, J. Non-Cryst. Solids 15 (3) (1974) 423–434.

[42] N.H. Ray, The structure and properties of inorganic polymeric phosphates, Br. Polym. J. 11 (4) (1979) 163–177.

[43] E. Metwalli, et al., Modifier effects on the properties and structure of aluminophosphate glasses, J. Non-Cryst. Solids 289 (2001) 113–122.

[44] R.D. Shannon, Revised effective ionic radii and systematic studies of interatomic distances in halides and chalcogenides, Acta Crystallogr. A32 (1976) 751–767.

[45] W.A. Weyl, et al., The constitution of glasses: a dynamic interpretation, Wiley and Sons, Fundamentals of the Structure of Inorganic Liquids and Solids, 1, Interscience Publishers, New York, 1962.

[46] J.F. Sarver, et al., Phase equilibria and manganese-activated fluorescence in the system Zn3(PO4) 2-Mg3(PO4)2, J. Electrochem. Soc. 106 (11) (1959) 960–963.

[47] F.L. Katnack, et al., Phase equilibria in the system ZnO–P$_2$O$_5$, J. Electrochem. Soc. 105 (3) (1958) 125–133.

[48] J.C. Knowles, Phosphate based glasses for biomedical applications, J. Mater. Chem. 13 (2003) 2395–2401.

[49] B.C. Sales, et al., Chromatographic studies of the structures of amorphous phosphates: a review, J. Non-Cryst. Solids 263&264 (2000) 155–166.

[50] J.R. Van Wazer, Phosphorus and its compounds, Chemistry, vol. 1, Interscience Publishers, Inc., New York, 1958.

[51] H. Takebe, et al., Compositional dependence of water durability in metaphosphate glasses, ICG, 2007, (Strasbourg, France).

[52] L. Popovic, et al., Correlation between Raman wavenumbers and P–O bond lengths in crystalline inorganic phosphates, J. Raman Spectrosc. 36 (2005) 2–11.

[53] B.N. Nelson, et al., Vibrational spectroscopy of cation–site interactions in phosphate glasses, J. Chem. Phys. 71 (7) (1979) 2739–2747.